Development of hydrogen-filled traveling-wave thermoacoustic engine for powering pulse-tube and traveling-wave refrigerators

M P Shenton, J W Leachman, and K I Matveev

HYdrogen Properties for Energy Research (HYPER) Center, School of Mechanical and Materials Engineering, Washington State University, Pullman, WA, 99164-2920, USA

Email: matveev@wsu.edu

Abstract. Current cryocooler technologies rely on compressors and displacers to generate pressure oscillations requiring high electrical power and regular maintenance intervals limiting the convenience of cryocoolers for renewable energy, specifically zero-boil-off applications. Thermoacoustic instabilities are spontaneously excited sound waves in resonators which transport energy along a piping network. Utilizing these sound waves to remove heat creates a robust paradigm for cryogenic refrigeration (cryocooling) with no moving parts. This study discusses the design of a thermoacoustic cryocooler using hydrogen as the working fluid. A toroidal acoustic resonator system is designed to excite traveling sound waves using an imposed temperature gradient on an engine regenerator between the ambient and hot heat exchangers. The generated acoustic waves then propagate into the pulse-tube or traveling-wave setup producing refrigeration in the cooler regenerator. Modeling techniques, results, and the optimal geometric configurations for the engine-refrigerator are reported. The geometric configurations are selected to minimize the temperature gradient in the engine core to reach a cryogenic temperature below 100 K and produce an acceptable COP at 110 K. A goal of this initial study is to establish the feasibility of this new cooling paradigm which can be scaled up to intercept heat leak in liquid hydrogen storage vessels.

1. Introduction

Current cryocooler cycles are predominantly the Gifford-McMahon and Stirling, both of which can include the Orifice Pulse-tube modification. These units utilize compressors, rotary valves, pistons, displacers, or linear motors to produce pressure oscillations to remove heat. Market cryocoolers achieve cooling capacities typically <100 W below 77 K but require two or more ~6-12 kW compressors to operate. Thermoacoustic oscillations are a promising alternative to the moving machinery currently driving these systems.

Thermoacoustic instabilities involve self-excited sound waves associated with the Raleigh criterion stating that acoustic motion of the fluid is encouraged when heat is added to the fluid during compression and removed when fluid is rarified [1]. Early experimental studies of these instabilities include the work of Higgins [2] producing oscillations using a hydrogen flame inside a tube and Sondhauss [3] exploring geometries observed during the process of glass blowing which generated sound. Thermoacoustic devices utilize porous matrices (regenerators) which enhance the inherent acoustic power produced due to these instabilities [4] and are categorized as either a standing-wave or

traveling-wave system. A standing-wave system relies on imperfect thermal contact between the porous material and the gas particles, when the pressure and velocity waves are out of phase, to convert thermal energy to acoustic energy. This is the working principle of the Sondhauss tube. A traveling-wave system utilizes in-phase pressure and velocity waves. Ceperley et al. [5] discussed thermodynamic similarities to Stirling cycles for traveling-wave thermoacoustic devices as depicted in section 2.1.

Yazaki et al. [6] measured acoustic amplitudes and temperature ratios across the stack and found that traveling-wave systems required smaller onset ratios than standing-wave configurations. Zare et al. [7] provides a review of traveling-wave systems and effective component design. Zinovyev et al. [8] simulated a traveling-wave system with helium as the working fluid using cryogenic temperatures. They calculated a reduction in the required temperature gradient for oscillations when using cryogenic temperatures rather than heating the system. Wang et al. [9] simulated a traveling-wave engine with helium as the working fluid using liquid natural gas in flow-through heat exchangers to produce the temperature gradient required for oscillations. Sun et al. [10] simulated and experimentally verified a three-stage coupled traveling-wave engine using liquid nitrogen to achieve the required temperature gradient. Los Alamos National Laboratory has produced several thermoacoustic engines which are summarized in Swift's textbook [4]. These prototypes usually employ a heating block and porous stack to enhance oscillations (often with helium as the working fluid) to produce useful acoustic power output [11, 12]. The traveling-wave prototype delivered 710 W with a Carnot efficiency of 41% using helium [12].

Thermoacoustic engines can be inverted into a thermoacoustic heat pump transferring energy from cold to hot reservoirs. Acoustic power is supplied, while the porous insert serves as media removing energy from the cold space. Jin et al. [13] review different thermoacoustic devices and working fluids. These works mention hydrogen mixtures, but do not analyze hydrogen as the sole working fluid. Shenton et al. [14] provides experimental measurements for hydrogen thermoacoustic oscillations (Taconis oscillations) in different pipe geometries to mitigate excitation in storage vessels. This study is motivated by the importance of long-term storage solutions for liquid hydrogen by eliminating boil-off losses [15]. This paper expands upon previous work by the authors and discusses modeling techniques and potential designs of an initial prototype that may later provide a robust and efficient cooling solution using a thermoacoustic engine installed outside a cryogenic tank, transferring acoustic power into a regenerator to remove heat from the stored liquid. The thermodynamic principles of a traveling-wave system as well as the development of a theoretical model analyzing system performance is described in Section 2. Section 3 presents calculations for different thermoacoustic devices including a traveling-wave engine, the traveling-wave engine connected to a pulse-tube, and a combined traveling-wave engine and refrigerator. Finally, the prototype design for fabrication of the traveling-wave engine is discussed in Section 4.

2. Thermodynamic and thermoacoustic theory of traveling-wave devices

2.1 Traveling-wave thermodynamic principles

A traveling-wave thermoacoustic cycle is similar to a Stirling cycle [5] where the working fluid oscillates through a porous matrix exchanging energy along the regenerator. The fluid particle is sufficiently close to the wall where the thermal and viscous penetration depths are larger than the hydraulic pore size ($\delta_{k,v} \gg r_h$). This promotes perfect thermal contact from the fluid particle to the regenerator wall. The penetration depths are calculated based upon the properties of the working fluid and are given as

$$\delta_k = \sqrt{\frac{2k}{\rho\omega c_p}}, \tag{1}$$

$$\delta_v = \sqrt{\frac{2\mu}{\rho\omega}}, \tag{2}$$

where the parameters μ, c_p, k, ρ, and ω are the viscosity, specific heat, thermal conductivity, density, and angular frequency, respectively.

In a traveling-wave engine, the fluid particle fluctuates through the regenerator from the cold side to the hot side, simultaneously undergoing expansion and gaining entropy in the form of heat from the wall. Then the fluid particle displaces through the regenerator from the hot to the cold side undergoing compression and loses entropy into the wall. This process is driven by the in-phase pressure and velocity waves traversing the regenerator. The temperature and position of the particle lag the pressure and velocity waves providing net flux of entropy streaming through the regenerator. A representation of this process and the associated thermodynamic state diagrams are shown in Figure 1.

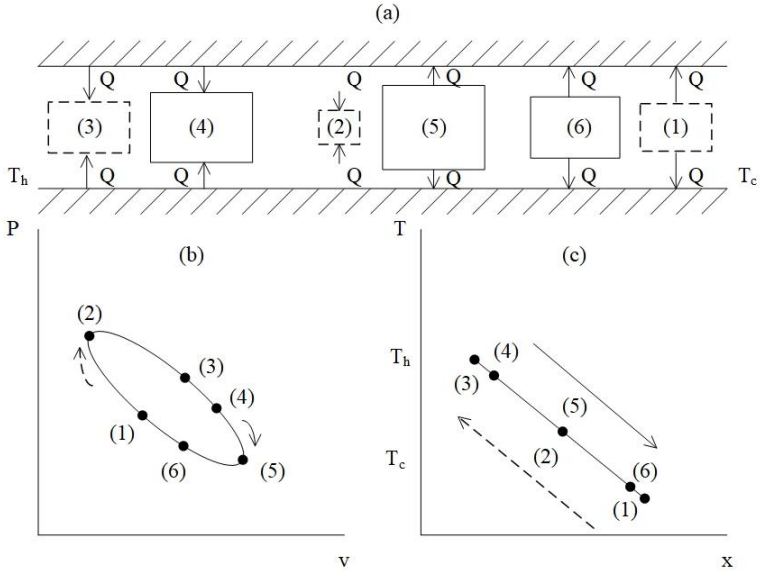

Figure 1. Fluid and thermodynamic representation of a traveling-wave system. (a) Fluid particle oscillating in a regenerator. (b) Pressure-specific-volume state diagram. (c) Temperature-position state diagram.

The area within the ellipsoid of the pressure-specific-volume represents the net work attributed to the cycle. The second law efficiencies of a thermoacoustic cycle are calculated as follows:

$$\eta_{II_{eng}} = \frac{W_a}{Q_H}\left(\frac{T_H}{T_H - T_c}\right), \tag{3}$$

$$\eta_{II_{ref}} = \frac{Q_c}{W_a}\left(\frac{T_H - T_c}{T_c}\right). \tag{4}$$

2.2 Governing equations of a thermoacoustic system

Modeling of a thermoacoustic apparatus can be executed using the program DeltaEC (Design Environment for Low-amplitude Thermoacoustic Energy Conversion) developed at Los Alamos National Laboratory [16]. This simulation package numerically solves the discretized governing thermoacoustic equations for a wide range of geometries and components,

$$\frac{dp_1}{dx} = -\frac{i\omega\rho_m}{A(1-f_v)}U_1, \tag{5}$$

$$\frac{dU_1}{dx} = -\frac{i\omega A}{\gamma p_m}\left[1 + \frac{(\gamma-1)f_k}{1+\epsilon_s}\right]p_1 + \frac{\beta(f_k - f_v)}{(1-f_v)(1-\sigma)(1+\epsilon_s)}\left(\frac{dT_m}{dx}\right)U_1. \tag{6}$$

In the employed equations, the oscillatory components of pressure (p') and the volumetric flow rate (U') are expressed as complex amplitudes (commonly used in acoustics), while the actual pressure and velocity fluctuations are given by the real parts,

$$p'(x,t) = Re[p(x)e^{i\omega t}], \quad (7)$$
$$U'(x,t) = Re[U(x)e^{i\omega t}]. \quad (8)$$

Thermodynamic variables T_m, ρ_m, and p_m are the mean (cross-section and time-averaged) temperature, density, and pressure of the fluid, γ is the specific heat ratio, and $\sigma = \mu c_p/k$ is the Prandtl number. The parameters μ, c_p, k, and β are the viscosity, specific heat, thermal conductivity, and thermal expansion coefficient of the fluid inside the tube, and A is the cross-sectional area. The correction factor ϵ_s accounts for temperature fluctuations in the tube wall material. The thermoacoustic functions f_k and f_v and ϵ_s depend on the geometry of the element and can be referenced from Swift's textbook or the DELTAEC manual [4, 16].

An approximation of a thermoacoustic device can be constructed using several elements (ducts, heat exchangers, stacks, etc.) represented as an acoustic circuit. After the system geometric configuration is created, the shooting method is applied to find solutions satisfying the boundary conditions defined by the user for the above one-dimensional equations.

3. Analysis of thermoacoustic engines and refrigerators

Three different configurations of a thermoacoustic device are presented including a traveling-wave engine, the traveling-wave engine connected to an orifice pulse-tube refrigerator, and a combination travelling-wave engine and refrigerator. All studies utilize hydrogen as the working fluid at 20 bar and are simulated with stainless steel as the engine construction material.

The thermoacoustic engine developed in this study has been modeled with 36 total elements encompassing two heat exchangers, a regenerator, elements for the toroidal tube network, and elements for the resonator network. The schematic used by DeltaEC is shown in Figure 2a which uses the 'MINOR' and 'IMPEDANCE' segments to account for the non-linear losses in the system. The additional parameters in the model account for non-linear acoustic losses, numeric result calculations, and the boundary conditions required both in the torus section and at the resonator end. The numbers in Figure 2a represent the elements input into DeltaEC, whereas the numbers in Figure 2b divide the traveling-wave engine into 12 main sections discussed below.

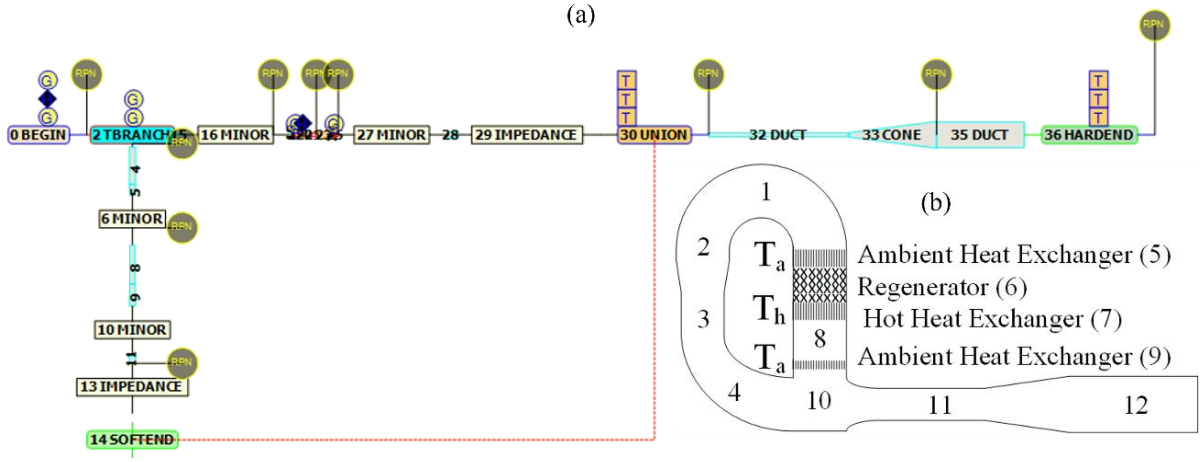

Figure 2. (a) Block diagram utilized in DeltaEC to model the traveling-wave engine. (b) Block diagram describing the primary components of the traveling-wave engine.

The geometric model of the system starts at the top of the first ambient heat exchanger designated as the begin block for acoustic parameters (Figure 2a). The next segment is designated as a T-branch which splits the flow path into 2 distinct sections. This branch accounts for the toroidal tubing network

(Figure 2b. sections 1-4) and the regenerator core (Figure 2b. sections 5-9). The toroidal tubing network consists of conical and constant diameter isothermal DUCT elements terminating in a SOFTEND element. The SOFTEND element acts as the connection point at section 10 (Figure 2b.) where the pressure and temperature of the system must be continuous. The regenerator core consists of STK elements which DeltaEC utilizes to calculate the temperature profile along the length of the tubing system. Three heat exchangers are described using the TX element. Finally, the core and the toroidal network are joined together using the UNION element with the proper boundary conditions mentioned above in the SOFTEND condition. The MINOR and IMPEDANCE blocks account for nonlinear acoustic losses with coefficients taken from Swift [4]. The rest of the model consists of the resonator network including an inertance tube and compliance volume connected by a conical duct at isothermal temperatures. A HARDEND boundary condition is implemented after the compliance to balance the energy transfer through the system and ensure zero velocity at the compliance wall.

Table 1. Inputs for the traveling-wave engine in DeltaEC.

Guesses	Targets
Acoustic frequency (Begin segment)	$Im\left(\frac{1}{Z}\right) = 0$ (Compliance)
Pressure amplitude at the top of the ambient heat exchanger (Begin segment)	$Re\left(\frac{1}{Z}\right) = 0$ (Compliance)
Real component of the impedance at the beginning of the loop (T-branch segment)	$\lvert p_1 \rvert_{union} = \lvert p_1 \rvert_{soft}$ (Union segment)
Imaginary component of the impedance at the beginning of the loop (T-branch segment)	$Ph(p_1)_{union} = Ph(p_1)_{soft}$ (Union segment)
Wattage input at the hot heat exchanger (HHX segment)	$T_{HHX} = input$ (HHX segment)
Wattage removed at the 1st ambient heat exchanger (1st AHX segment)	$T_{union} = T_{soft}$ (Union segment)
Wattage removed at the 2nd ambient heat exchanger (2nd AHX segment)	$H_{tot} = 0\ W$ (Compliance)

Table 1 lists the input guesses and targets for the model. These parameters ensure that boundary conditions are met by varying the guesses until convergence of the targets is satisfied. For this thermoacoustic engine, the guesses include frequency, pressure amplitude, and heat transfer rates through the heat exchangers as well as the impedance where the toroidal section connects. The targets include ensuring that all energy is balanced throughout the system and is dissipated at the end of the resonator, the rigid wall condition is met at the end of the resonator (enforced through the zero-inverse impedance), and the pressure amplitude, pressure phase, and temperature at the connection for the toroidal tubing network is continuous. After the model converged, parametric studies were conducted on the geometry of the system to find a configuration that produced acoustic power to drive a refrigerator cooling to 100 K.

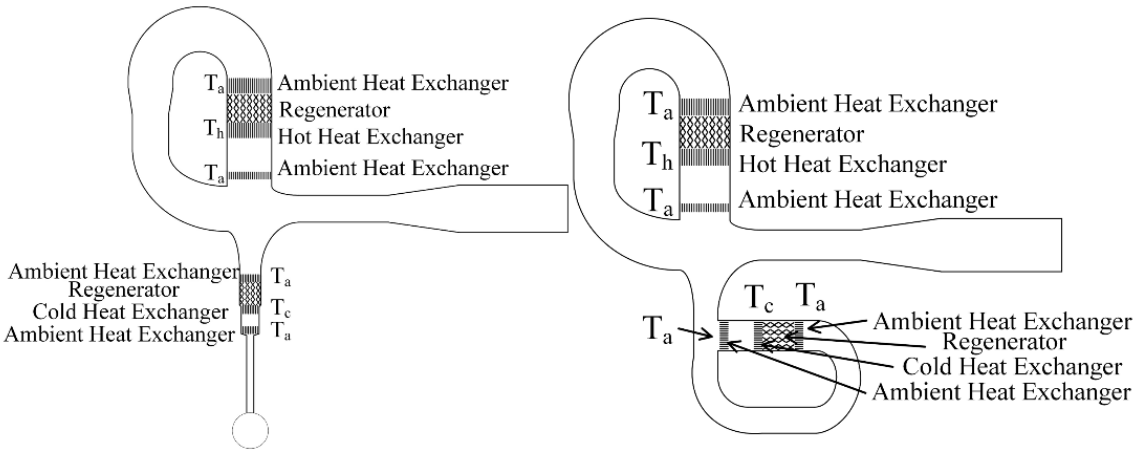

Figure 3. Schematics of a: (Left) Traveling-wave engine connected to an orifice pulse-tube. (Right) traveling-wave engine connected to a traveling-wave refrigerator.

The schematics of the refrigerator sections connected to the engine are shown in Figure 3. These refrigerators are parameterized using similar elements in DELTAEC with additional guesses and targets to ensure continuity at the end of the pulse-tube compliance and at the connection in the traveling-wave refrigerator. The important parameters for these systems include the temperature gradients, the acoustic power, and the heat loads on the hot heat exchanger and the cold heat exchanger. These values are utilized to calculate the efficiency of the system using equations 3-4. The results are shown in Table 2. When parameterizing the engine, the heat load at the hot heat exchanger was kept constant at 324 W. This led to a hot temperature equaling 656 K and an efficiency of 39%. Once the refrigerators are included in the simulations, the acoustic power reported in the table is the fraction of power that is flowing into the refrigerator section. In addition, the hot and cold temperatures were kept as similar as possible at 815 K and ~105 K respectively, to compare the different systems. The coldest temperature with the pulse-tube setup is 107 K with a heat input of 399 W. The traveling-wave system reaches 105 K with a heat input into the engine of 324 W. The final simulation included a heat load on the cold heat exchanger to determine the cooling capacity. The cold temperature is kept constant at 150 K to determine how much heat can be lifted. For the pulse-tube setup, the heat lift is approximately 6 W consuming 34 W of acoustic power with a calculated 2nd-law efficiency of 17%. For the traveling-wave refrigerator, the heat lift is 8 W for an acoustic power consumption of 27.2 W. The 2nd-law efficiency increases to approximately 29%. This indicates that a combined traveling-wave system is more efficient while providing cryogenic cooling with no moving parts.

Table 2. Parametric results for the hydrogen thermoacoustic system. (TWE – traveling-wave engine, OPTR - orifice pulse-tube, TWR- traveling-wave refrigerator.)

Parameter	Device TWE	TWE_OPTR	TWE_TWR	TWE_OPTR	TWE_TWR
$\frac{P_1}{P_m}(-)$	0.07	0.07	0.06	0.08	0.06
$f\ (Hz)$	149	147.2	156.8	147.2	156.8
$T_H\ (K)$	656	815	815	815	815
$T_c\ (K)$	-	107	105	150	150
$Q_H\ (W)$	324	399	324	421	351
$Q_c\ (W)$	-	0	0	5.9	8.0
$W_a\ (W)$	80.2	37.6	30.4	34.4	27.2
$\eta_{II}\ (-)$	0.39	-	-	0.17	0.29

4. Experimental traveling-wave engine

Using the modeling results discussed above, a design of the hydrogen thermoacoustic traveling-wave engine was developed and shown in Figure 4. The hot heat exchanger will be constructed as a porous stainless-steel insert press fit into the tube below the regenerator. Two different heat methods are explored, including conventional cartridge heaters and novel induction methods for thermal generation along the pores. Different mesh screen sizes and hydrogen compatible materials will be utilized to validate the model and optimize performance in the regenerator. The temperature decreases to ambient conditions at both ambient heat exchangers. The rest of the system is assumed isothermal at ambient conditions. Thermocouples and dynamic pressure transducers are placed along the core of the system to measure acoustic pressure amplitude, phase and the temperature gradient. The acoustic power splits at the cross connection with a portion dissipating in the resonator, traversing through the torus, or being utilized by the load. Initial testing will isolate the load tube so that all energy is dissipated in the resonator and torus. The resonator inertance and compliance are connected at the cross section and extend to a plate attaching the gas inlet and vent lines as well as pressure relief devices. This experimental setup will be constructed and utilized to demonstrate a combined hydrogen thermoacoustic engine and refrigerator with no moving parts.

Figure 4. Conceptual rendering of the traveling-wave engine.

5. Conclusion

This study provides a framework for calculating traveling-wave thermoacoustic devices. Additionally, a hydrogen thermoacoustic traveling-wave engine has been designed to investigate the potential of using no moving parts to eliminate boil-off losses in liquid hydrogen storage vessels. Calculations for the prototype indicate the ability to reach 100 K for both standing-wave and traveling-wave refrigerators while providing evidence of an increase in efficiency for the traveling-wave system. The thermoacoustic modeling results will be verified with the experimental setup using hydrogen at 20 barg pressure. While the current calculations don't indicate a large capacity of useful cooling at 100 K, this design provides a baseline for designing a hydrogen thermoacoustic system to be scaled and optimized. The next steps involve manufacturing the thermoacoustic system elements. Experimental measurements will be taken to compare with the theoretical predictions for this cooler.

Acknowledgements

This research was supported in part by the U.S. National Science Foundation, grant number 2214235. We also extend our gratitude to Jan Schonander for his help in the design calculations and CAD generation of the traveling-wave engine prototype.

References

[1] Rayleigh J 1896 *The theory of sound. vol. I and II.* (New York: Dover Publications)
[2] Putnam A A and Dennis W R 1956 *The Journal of the Acoustical Society of America.* **28** 246-259
[3] Sondhauss C 1850 *Annalen der Physik.* **155** 1-34
[4] Swift G W 2003 *Thermoacoustics: A unifying perspective for some engines and refrigerators.* (Mellville, NY: Acoustical society of America)
[5] Ceperley P H 1979 *The Journal of the Acoustical Society of America.* **66** 1508-1513
[6] Yazaki T, Iwata A, Maekawa T and Tominaga A 1998 *Physical Review Letters.* **81** 3128
[7] Zare S, Tavakolpour-Saleh A, Aghahosseini A and Mirshekari R 2023 *International Journal of Green Energy.* **20** 89-111
[8] Zinovyev E, Vorotnikov G, Nekrasova S and Sarmin D 2022 *7th Asia Conference on Power and Electrical Engineering (ACPEE)*
[9] Wang K, Dubey S, Choo F H and Duan F 2017 *Energy.* **127** 280-290.
[10] Sun D, Zhang J, Pan H, Shen Q, Qi Y, Qiao X and Su S 2021 *Cryogenics.* **120** 103385.
[11] Swift G W 1992 *The Journal of the Acoustical Society of America.* **92** 1551-63
[12] Backhaus S and Swift G W 2000 *The Journal of the Acoustical Society of America*. **107** 3148-3166
[13] Jin T, Huang J, Feng Y, Yang R, Tang K and Radebaugh R 2015 *Energy.* **93** 828-853
[14] Shenton M P, Leachman J W and Matveev K I 2024 *Cryogenics*. **143** 103940
[15] Leachman J W, Wilhelmsen Ø and Matveev K I 2025 *Cool Fuel: The Science and Engineering of Cryogenic Hydrogen*. (Oxford, England: Oxford University Press)
[16] Clark J P, Ward W C and Swift G W 2007 *The Journal of the Acoustical Society of America*. **122** 3014